



A 3D printed human upper respiratory tract model for particulate deposition profiling

Seng Han Lim^{a,1}, Sol Park^{b,1}, Chun Chuan Lee^a, Paul Chi Lui Ho^a, Philip Chi Lip Kwok^b, Lifeng Kang^{b,*}

^a Department of Pharmacy, National University of Singapore, 18 Science Drive 4, Block S4A, Level 3, Singapore 117543, Republic of Singapore

^b School of Pharmacy, Faculty of Medicine and Health, University of Sydney, Pharmacy and Bank Building A15, NSW 2006, Australia

ARTICLE INFO

Keywords:

3D printing
Upper respiratory tract model
Fused deposition modelling
In vitro-in vivo correlation
Salbutamol
Inhalation

ABSTRACT

Pulmonary route is the main route of drug delivery for patients with asthma and chronic obstructive pulmonary diseases, offering several advantages over the oral route. Determining the amount of drug deposited onto various parts of the respiratory tract allows for a good correlation to clinical efficacy of inhalation drug devices. However, current *in vitro* cascade impactors measure only the aerodynamic particle size distribution, which does not truly represent the *in vivo* deposition pattern in human respiratory tract. In this study, a human upper respiratory tract model was fabricated using a 3D printer and subsequently characterized for its dimensional accuracy, surface finishing and air leaking. The effects of using a spacer and/or various airflow rates were also investigated. To assess this *in vitro* model, the deposition pattern of a model drug, namely, salbutamol sulphate, was tested. The resultant deposition pattern of salbutamol sulphate from a metered dose inhaler at 15 L per minute with the spacer, showed no significant difference from that of a published radiological *in vivo* study performed in adult humans. In addition, it was also found that the deposition pattern of salbutamol at 35 L per minute was comparable to the results of another published study in human. This *in vitro* model, showing reasonable *in vitro-in vivo* correlation, may provide opportunities for personalized medicine in special populations or disease states.

1. Introduction

Pulmonary drug delivery refers to the inhalation of drug particles via the oral or nasal cavity into the respiratory tract (Fig. 1A) consisting of the upper airways (i.e., the nasal cavity, oral cavity, pharynx, and larynx) and the tracheobronchial tree (i.e., the trachea, bronchi, bronchioles, alveolar ducts, alveolar sacs, and alveoli) (Ruigrok et al., 2016). This is achieved typically with mechanical devices such as pressurised metered dose inhaler (pMDI), dry powder inhaler (DPI) or nebulizer. It is also the main route of drug delivery for lung-related diseases, such as asthma and chronic obstructive pulmonary disease (COPD). This local delivery to the lungs allows the use of small drug doses and reduces potential systemic adverse effects (Labiris and Dolovich, 2003a, b). Increasingly, pulmonary drug delivery has also been used for systemic administration due to its quick onset of action attributed to the large surface area for absorption, rich network of vasculature and thin air-blood barrier in the alveolar region. Furthermore, it can bypass

barriers of drug absorption such as poor gastrointestinal absorption and first-pass metabolism in the liver (Gandhimathi et al., 2015; Hess, 2008; Ibrahim et al., 2015; Liang et al., 2015). Due to the advantages, it is no surprise that pulmonary route of drug delivery took up >20% of the drug delivery mode in global markets (Gandhimathi et al., 2015). However, all these therapeutic effects can only be achieved if the drug particles are deposited in the desired parts of our respiratory tract (Chow et al., 2007; Kim et al., 2015).

Deposition of drug particles in the respiratory tract is governed by key mechanisms including inertial impaction, gravitational sedimentation and Brownian diffusion (Heyder et al., 1986). An interplay of factors affects the eventual particle deposition within the respiratory tract. These factors include 1) formulation parameters, such as particle size, density, shape (Yang et al., 2014); 2) ventilatory parameters, such as tidal volume, inspiratory flow rate and breath hold time (Katz et al., 2001); and 3) human factors, such as posture (Sa et al., 2015), lung surface morphology (Oakes et al., 2014), type of inhalers used and user

* Corresponding author at: School of Pharmacy, Faculty of Medicine and Health, University of Sydney, Pharmacy and Bank Building A15, Science Rd, NSW 2006, Australia.

E-mail address: lifeng.kang@sydney.edu.au (L. Kang).

¹ These authors made equal contributions.

<https://doi.org/10.1016/j.ijpharm.2021.120307>

Received 4 September 2020; Received in revised form 19 January 2021; Accepted 20 January 2021

Available online 1 February 2021

0378-5173/© 2021 Elsevier B.V. All rights reserved.

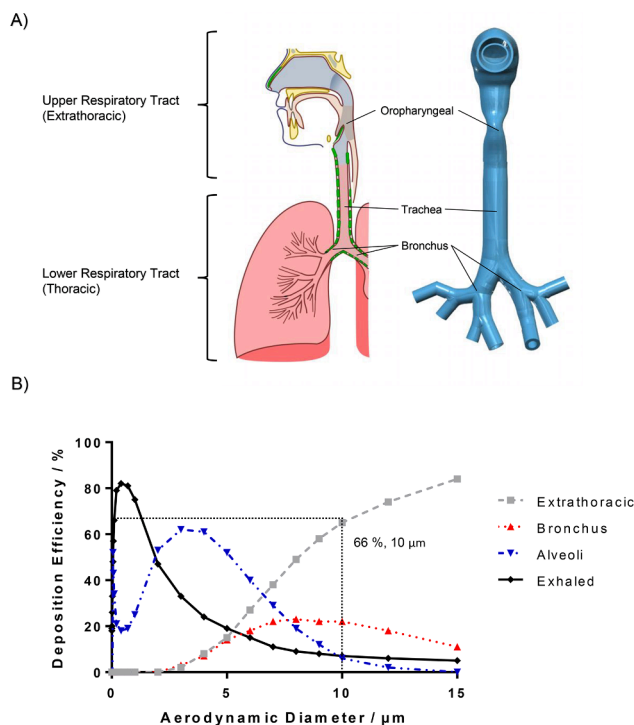


Fig. 1. Schematic of HURT Model Assembly & *In Vivo* Deposition Efficiency of Inhaled Particles in HURT. A) illustrates a brief schematic of the HURT anatomy, followed by the 3D model of adult HURT anatomy (Wikimedia, accessed, 18/01/, 2021). B) illustrates the deposition efficiency of inhalable particles at various region of a healthy male respiratory tract. BLACK dotted line indicates that only 66% of 10 μm inhalable particles is deposited in the extra thoracic region, in contrast to the general correlation that all 10 μm particles will be deposited in the extra thoracic region (Laube et al., 2011).

competency in inhaler technique (Brand et al., 2008). To effectively measure the deposition of inhaled particles within the respiratory tract, several strategies have been established and can be broadly classified into *in vivo*, *in silico* and *in vitro* strategies.

Often regarded as a gold standard, *in vivo* strategy uses a range of three-dimensional (3D) imaging techniques, such as single photon emission computed tomography (SPECT) or magnetic resonance imaging (MRI) to monitor the deposition of particles in animals or human subjects (Fleming et al., 2015; Greenblatt et al., 2015; Majoral et al., 2014; Oakes et al., 2014; Thompson and Finlay, 2012). While this method of measurement can provide clear evidence for the deposition of inhaled particles, it is often tedious for both the administrator and human subject. Furthermore, radiation-based imaging techniques, such as SPECT, expose the human subjects to radiations that are not well suited for special populations, including the paediatrics, geriatrics and pregnant women.

As an alternative to *in vivo* strategy, *in silico* or mathematical models were developed and validated against *in vivo* experimental data (Fernandez Tena and Casan Clara, 2012; Katz et al., 2001; Segal et al., 2000; Stuart, 1976; Sturm, 2016). While this approach has been increasingly adopted, it is nonetheless an indirect measurement of the deposition of inhaled particles. The accuracy of its prediction is limited by the direct measurable parameters.

The third class of strategies involve the use of *in vitro* cascade impactors, such as the Andersen Cascade Impactor or Next Generation Impactor. These devices measure the aerodynamic diameter (ADD) of drug particles, which has been deemed as the most relevant parameter used to describe the inhaled drug particles (Guo et al., 2008). Inhaled aerosols with a mass median aerodynamic diameter (MMAD) of 1–5 μm are considered as respirable by humans and can be deposited in the

alveoli for absorption (Fernandez Tena and Casan Clara, 2012; Taki et al., 2010). Furthermore, cascade impaction tests have been widely used for assessing the delivery characteristics of pMDIs and DPIs and is a mandatory parameter to be reported for all inhalation product development studies (EMA, accessed 18/01/, 2021). Typically, cascade impaction tests for pMDIs have been conducted using the cascade impactor with a United States Pharmacopeia induction port to serve as an inlet for inhalers.

However, both ADD and MMAD have their limitations. As shown in Fig. 1B, for a monodispersion of ADD 10 μm , it is not entirely deposited in the extrathoracic region as expected, due to its large ADD. Instead, only about 66% of the particles are deposited in the extrathoracic region, with up to 10% of the particles eventually depositing in the alveoli region (Laube et al., 2011).

This variation may be due to the insufficiency of cascade impactor to account for deposition mechanism other than inertial impaction. The airway geometry, which is not accounted for in traditional impactors, may contribute significantly to the deposition of inhaled particles (Feng et al., 2017). However, it is difficult to develop a model to replicate airways, due to the complex geometry in the human throat and oropharyngeal region.

In recent years, the Alberta Idealised Throat model was also developed to have a more realistic representation of the upper airway (Lewis et al., 2016). The Alberta Idealised Throat model mimics the upper human respiratory tract and replicates *in vivo* particle deposition. Although this model has been commonly used, a major drawback is found in its simplified design (Zhang et al., 2006). As the name suggests, the model only mimics the oropharynx, limiting the usefulness of this model.

To address this issue, 3D printing may be used. 3D printing is an additive manufacturing technology based on computer-aided designed (CAD) to create a complex 3D geometry (Goole and Amighi, 2016). The increasing diversity of materials used in different 3D printing techniques enables the fabrication of microscale structures made of polymers, ceramics or metal (Liu et al., 2013). Furthermore, 3D printing offers opportunities for personalisation or fabrication of organic shapes, due to its ability to translate medical body scans into CAD models that can be printed into actual objects (Chen et al., 2020; Lim et al., 2018). Together with the cost reduction of 3D printing technologies over the last few years due to expiry of patent (Kim et al., 2016), 3D printing has become an important tool.

The growing emphasis on studying infectious respiratory tract diseases, such as Coronavirus, further highlights the potential role of 3D printing. Many infectious respiratory tract diseases are rapidly transmitted from person to person through contact with an infected individual's cough or sneeze droplets (Fehr and Perlman, 2015). Thus, 3D printing can be an inexpensive method of manufacturing models to be used in research.

The application of 3D printing in pulmonary medicine has become significantly popular over recent years. Zhao et al., created a lung phantom with radio frequency ablation indicator using 3D printing based off of medical images (Zhao et al., 2018). This model was developed to accurately test new tools and devices and help pulmonologists practice endobronchial interventions. Xi et al., also developed a 3D printed human upper respiratory model and observed the deposition distribution of nebulized aerosols (Xi et al., 2018). Two inhalation rates and three types of nebulizers were utilised, and it was determined that the greatest particle deposition was at 10 L/min flow rate. In 2019, Asgari et al., 3D printed a model which replicated physiological thermal conditions of a human respiratory tract by embedding water capillaries into the walls (Asgari et al., 2019). The cast was specifically designed for air flow and aerosol deposition experiments. Recently in 2020, Kolewe et al., 3D printed lung models based on a healthy 47-year-old male (Kolewe et al., 2020). These lung models were then used to study lobe targeting. Also in 2020, Tabe et al., developed a 3D lung model to study different airflow rates (Tabé et al., 2020).

As illustrated, several studies have investigated particle deposition using 3D printed models, however, none of these studies have thoroughly investigated particulate drug distribution in a 3D printed human upper respiratory tract (HURT) model with controlled flow rates. Thus, we developed a HURT assembly, comprising larynx, trachea, and part of bronchus, to determine the deposition of inhaled drug particles in respiratory tract. The results obtained from the 3D printed model are compared with those from previous human studies. To our knowledge, this HURT model is the first to replicate the structure of a real human respiratory tract from the mouth to the bronchi for *in vitro* dry particle deposition testing.

2. Materials and methods

2.1. Materials

All mentions of water in this article refers to deionised water, filtered from a Millipore system, unless otherwise stated. Salbutamol sulfate standard and acetone were purchased from Sigma Aldrich (Merck, KGaA, Darmstadt, Germany). Ventolin® Evohaler (GlaxoSmithKline, Brentford, UK), containing 100 µg of salbutamol sulphate per puff, and

the Aerochamber Plus® Flow-Vu® spacer mouthpiece were purchased from a local pharmacy in Singapore. Acrylonitrile butadiene styrene filament was purchased from XYZprinting, Inc (San Diego, California, USA).

2.2. Overview of device setup

With reference to Fig. 2A, a total of five parts were identified for the entire device setup, namely (i) Inhaler inlet, (ii) HURT assembly, (iii) Pass-through filter, (iv) Air flow meter and (v) Vacuum pumps (RV 3, Edwards, Burgess Hill, England, UK). Within the HURT assembly, the oropharyngeal, tracheal and bronchial regions were demarcated in Fig. 2A. Pass-through filter was created to simulate that of the alveolar region. Throughout the setup, an airflow is generated by the suction force of the lab scale vacuum pump, connected to the setup via flexible polyvinyl chloride (PVC) tubing. All particles deposited within the tubing were also considered part of the alveolar region. The rate of airflow is controlled using an air-flow meter and adjusted to simulate various respiratory minute volume during different activities of daily living (15 L per minute (LPM), 25 LPM and 35 LPM). An inhaler fitting was specially designed to ensure perfect fit between standard Evohaler

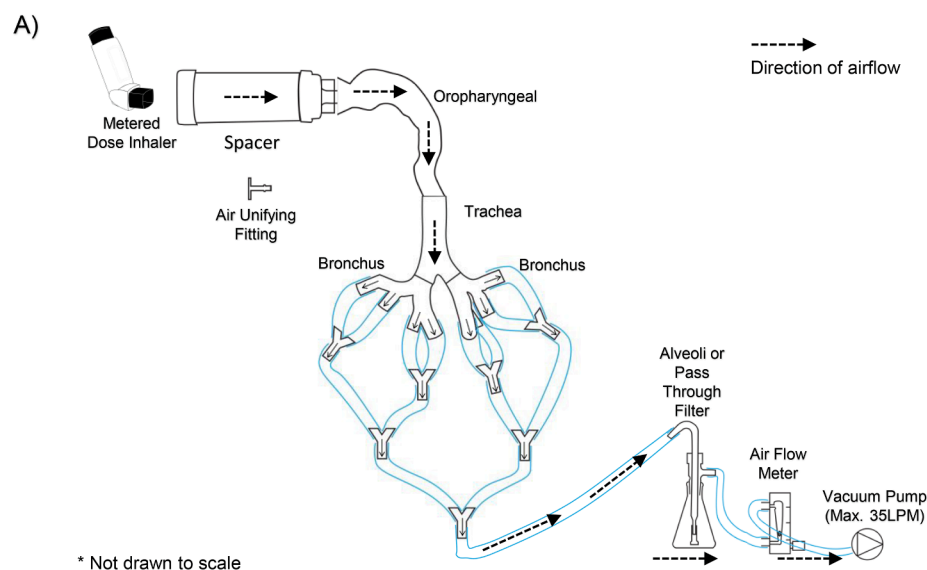
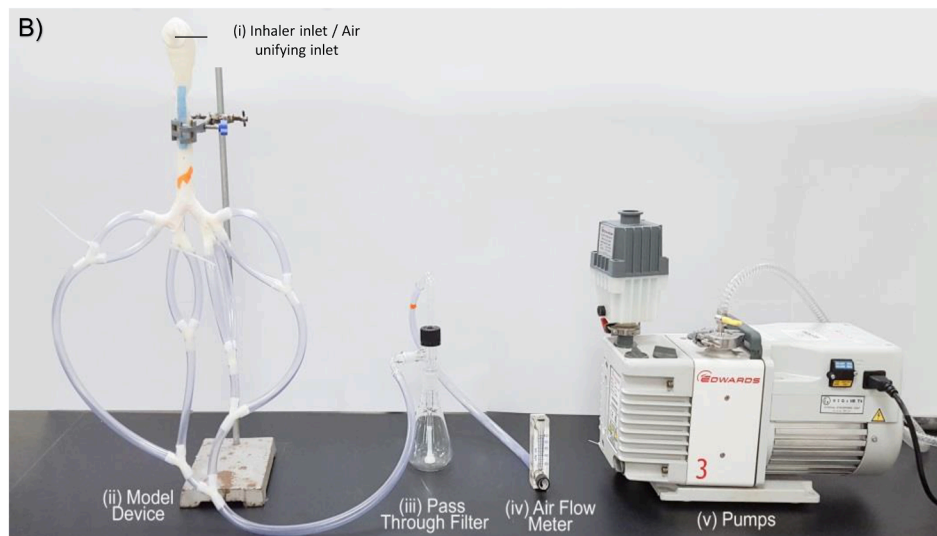


Fig. 2. Overall Device Setup. A) shows the general schematic of the setup, starting from the aerochamber which connects the inhaler to the device. The device is modelled after the human lung consisting of the oropharyngeal, trachea, bronchus and finally the alveoli. The flow of air through the device is generated by a vacuum pump and regulated through the use of an air flow meter. B) shows the actual setup of testing device for the deposition studies. The 5 major components of the setup are illustrated in the figure.



mouthpiece and the oropharyngeal region. This was used for the deposition of salbutamol sulfate particles from a commercial Evohaler. To better simulate actual clinical scenario where many geriatrics or paediatrics used a spacer (Aerochamber®), to aid inhalation, the particle deposition tests were also repeated with the use of a spacer, together with the Evohaler. When measuring the air seal of the entire device, an air unifying fitting was used instead. Two sets of lung model assembly (Model A and B) were fabricated and used throughout the study. Fig. 2B illustrates the actual setup of HURT assembly using the printed model and other simple laboratory equipment.

2.3. Acquisition and design of HURT model assembly

Computer aided design (CAD) files of adult human lung anatomy were obtained from Respiratory Drug Delivery Online (RDDOnline, accessed 18/01/, 2021). The *in vitro* model consists of HURT down to the third generation. The mouth to throat geometry is the elliptical model proposed by Xi and Longest (Xi and Longest, 2007) and contains the oral cavity, pharynx, and larynx. This geometry is based on the oral airway cast reported by Cheng et al. (Cheng et al., 1997) and in-house computed tomography (CT) data of the pharynx and larynx. The remaining portion of HURT was based on the anatomical cast dimensions of a 60 year old, 80 kg adult male with no lung abnormalities, reported by Yeh and Schum (Yeh and Schum, 1980) and scaled to a functional residual capacity of 3.5 L. Briefly, to generate the realistic model, a virtual 3D airway geometry was created based on the CT data of a healthy adult imaged using a multi-row helical scanner with a slice thickness of 1 mm. Image files were then converted to a solid body model using the software package Materialise Interactive Medical Image Control System (MIMICS) (Materialise, Ann Arbor, MI, USA). The surface geometry was imported into ANSYS Integrated Computer-aided Engineering and Manufacturing (ICEM) (ANSYS, Inc., PA, USA) as an Initial Graphics Exchange Specification (IGES) file for meshing. These models were designed to test aerosol deposition, flow field characteristics, or for the construction of computational fluid dynamics (CFD) geometries (Delvadia et al., 2012; Tian et al., 2011a; Tian et al., 2011b; Xi and Longest, 2007, 2008). The bronchus models were modified slightly to allow for easy separation and connection of tubing for a leak-proof flow of air to simulate lung respiration. This was achieved using a combination of three programmes, namely 3D Builder® (Microsoft®, USA), Solidworks® 2016 (Dassault Systemes®, France) and Autodesk® Netfabb® (Autodesk™ Inc., USA). The CAD model was finally converted to a stereolithography (STL) file and sliced using Simplify3D® (Cincinnati, OH, USA) with customized support before transferring to the 3D printer for fabrication.

2.4. 3D printing of HURT

All 3D printings of the HURT were performed with a fused deposition modelling (FDM) 3D printer (Davinci 1.0, XYZprinting Inc., CA, USA), with natural-coloured acrylonitrile butadiene styrene (ABS) filament. Briefly, in FDM 3D printing, an ABS filament of 1.75 mm diameter was passed through a heated nozzle of 210 °C. The heat softened the ABS, which was then extruded and deposited onto a glass build plate. The glass build plate was heated up to 90 °C to prevent premature cooling of the deposited ABS that might result in warpage. Sequential layers of the deposited and hardened ABS were then built up to create an object in three dimensions, as determined by the CAD model. All parts of the model were printed with a set of pre-optimised parameters to ensure the prints were acceptably smooth, accurate and airtight (Table 1). These parameters included printing speed, infill density, support structures and orientation of print. Support structures were removed with a standard plier from the printed object before any further processing was performed. Three sets of HURT assembly were fabricated, but only two sets of HURT assembly (Model A and B) were used for the study to strike a balance between replicability and quick changeover.

Table 1

Pre-optimized printing parameters for HURT model.

	Oropharyngeal	Trachea & Bronchus
Extruder temp. @ layer 1 & 2 (°C)	225	225
Extruder temp. @ > layer 2 (°C)	210	210
Bed temp. (°C)	90	90
Nozzle diameter (mm)	0.4	0.4
Layer height (mm)	0.2	0.2
Printing speed (mm/s)	40	60
Infill density (%)	30	20

In all 3 models, temperature of extruder was held at a standard 210 °C for all printing done at layer 3 and above. However, to provide better adhesion of the model to print bed (held at 90 °C throughout the print job), the temperature of extruder was elevated to 225 °C for the 1st two layers of each model. A standard 0.4 mm diameter nozzle was used for the extrusion of filament at a layer height of 0.2 mm. This intermediate layer height provided a good balance between resolution and the duration of print. Finally, both trachea and bronchus were printed at 60 mm/s with an infill density of 20%, while the oropharyngeal was printed at 40 mm/s with an infill density of 30%. The main contributing factor for these differences was due to the larger size of oropharyngeal and also the overhanging and curved structures of the oropharyngeal which would benefit from a slower printing speed at a higher infill density, in order to achieve a dimensionally accurate print.

2.5. Post processing (acetone vapour polishing)

The ABS prints were first examined for any visible defects or roughness after printing. Any defective prints were discarded and reprinted. Subsequently, two printed models were placed in a cylindrical container (height = 13 cm, radius = 8 cm) of volume 2.613 L. Twenty millilitres of acetone was added to standard C-fold paper towel affixed at the perimeter of container to ensure uniform acetone vapour polishing. The container was enclosed for a duration of 2 h, to allow the acetone to vaporise and saturate the container. During treatment, acetone vapour smoothed out any uneven surfaces of the prints by partially dissolving the surface ABS. After 2 h, the container was vented for 30 min, before the next batch of printed objects were placed within the container for acetone vapour polishing. Flat bronchus, tangent bronchus and oropharyngeal prints were treated before the trachea. After treatment of the trachea, all the polished parts were manually fitted together. The joints were then tightened and sealed with Parafilm® (Bemis, USA) before being left to dry for 2 days in a standard laminar flow fume hood. The final printed parts were then measured physically using a ruler and compared to the original CAD model to determine the accuracy and precision of 3D printing.

2.6. Water contact angle for printed object

2 cm × 2 cm × 5 mm ABS plate were printed for the measurement. The printed plates were either treated with acetone vapour, sanded with coarse sandpaper or left untreated. Each of the plates were then subjected to water contact angle test using micropore deionized water. The contact angle of water droplet was measured via Video Contact Angle (VCA) System-Optima from AST Products.

2.7. Microscopy

Both post processed and unprocessed ABS printed square cubes were used for imaging under standard procedures of a field emission scanning electron microscope (FESEM) (JSM-7610F, JEOL, Tokyo, Japan). Briefly, each of the samples are coated with a thin layer of platinum using a standard sputter coater for 30 s and mounted onto the FESEM stub, before being viewed under a voltage of 5 kV, emission current of 10 µA, working distance of 8 mm using LEI detector and a vacuum pressure

of at least 1.91×10^{-4} Pa. Images of drug particles were captured using a SMZ 1500 stereomicroscope (Nikon, Tokyo, Japan). Any other images were captured using a standard handphone camera.

2.8. Air seal test

Before each deposition test, airflow before the inhaler inlet and after the HURT assembly model was measured and recorded. A maximum allowable limit of 20% drop in airflow between the two sites was implemented. The final setup was sealed with tape, hose clamp, cable tie, vacuum grease and parafilm to achieve an airtight seal. Air seal was also used to ensure that results obtained from the two sets of HURT assembly could be compared.

2.9. Recovery of particle deposition test

The recovery of each particle deposition test was calculated by dividing the total amount of drug recovered from all parts of HURT assembly against the total number of puffs multiplied by the dose of drug for each puff. A consistent and similar recovery between the two sets of HURT assembly ensured that their deposition results were comparable.

2.10. Evaluation of pressurised metered dose inhaler (pMDI)

Salbutamol sulphate pMDI (Ventolin® Evohaler, GlaxoSmithKline, Brentford, UK) was sprayed onto a glass slide kept in 50 mL Falcon tube. The setup is being left stagnant for any airborne particle to settle for 5 min. The glass slides loaded with particles was subsequently imaged under an optical microscope (SMZ 1500, Nikon, Tokyo, Japan). Using imaging software NIS-Elements D 4.30.00 (Nikon, Tokyo, Japan), the longest diameter and tangential diameter of the particles were measured for the evaluation of particle size distribution. A total of 808 particles were counted and the calculated volume median aerodynamic diameter (VMAD) was obtained. ADD was calculated using the below formula:

$$ADD = \left(\text{Longest diameter} + \text{Tangential diameter} \right) \div 2 \times \sqrt{\text{True density of salbutamol sulphate particle}}$$

Where the true density of salbutamol sulphate is 1.3 g cm^{-3} (Chiou et al., 2007)

2.11. Airway drug deposition study for salbutamol sulphate (Ventolin® Evohaler)

At the beginning of each particle deposition test, 15 mL of water was first introduced into the pass-through filter chamber. The vacuum pump was then started at the desired airflow of either 15 L per minute (LPM), 25 LPM or 30 LPM. A 30 s interval was provided to allow the stabilisation of airflow before the first spray from the pMDI was administered. A 10 s interval was given between each spray to allow for complete deposition of salbutamol sulphate into the HURT assembly. A total of 10 sprays were administered. An additional 30 s after the last administered dose was given to allow complete particle deposition. All parts of the HURT assembly were then dismantled and removed from each other. Spacer and oropharyngeal region were thoroughly washed with 10 mL of water each. Trachea, flat bronchus and tangent bronchus was washed with 5 mL of water each. All the connecting tubing after the HURT assembly up to the pass-through filter were washed with 15 mL of water present in the pass-through filter earlier. All the different washed out solution were subsequently quantified using a UV spectrometer (U-1800, Hitachi, Japan) and salbutamol sulfate standard solutions. All parts of the HURT assembly were cleaned and dried thoroughly before

the next run. All experiments were carried out in triplicates.

2.12. Statistical analysis

All data were collated and prepared using GraphPad Prism 6 (GraphPad Software Inc, CA, USA) for any graphical outputs. All experiments were conducted in triplicates and the results presented as mean \pm standard deviation. Statistical analysis was performed by one-way analysis of variance followed by Tukey *post hoc* test using IBM SPSS Statistics 21.0 (IBM, New York, USA). A probability value of p less than 0.05 was considered statistically significant.

3. Results

3.1. 3D printed HURT assembly model

Using the set of pre-optimised printing parameters, the HURT model was successfully printed, compartment by compartment. No visible defects were observed after 3D printing. Physical measurement of the final printed parts (Fig. 3) demonstrated reasonable accuracy and precision for FDM 3D printing in the fabrication of the HURT assembly. All dimensions of the various compartment were within 10% error, with a tendency for smaller parts to have a higher percentage error. Printed HURT assembly was also sturdy and lightweight due to the use of ABS as its printing material. Support structures were thinly printed and can be easily removed manually. For supports structures that cannot be removed with hands alone, pliers were enough to remove them easily.

3.2. Effect of post processing on surface properties of HURT assembly model

Post processing of the printed parts using acetone vapour resulted in a drastically improved appearance. Other than becoming reflective and glossy in appearance, the treated parts had a smoother appearance. The

layering appearance due to additive nature of 3D printing were removed, as illustrated in Fig. 4A. The layered surface before post processing could have resulted in premature deposition of the inhaled particles due to surface roughness and increased surface area. Therefore, it was necessary to ensure a smooth inner surface for all compartments of the HURT assembly model. In Fig. 4B, water contact angle of ABS surfaces post processed using different methods were illustrated. The similar water contact angle demonstrated no significant effect of acetone treatment on the hydrophobicity of ABS. However, from the small standard deviation (SD) demonstrated in Fig. 4Bi as compared to Fig. 4Bii and Fig. 4Biii, it can be inferred that the ABS surface treated with acetone vapour was much smoother and consistent as compared to ABS with no treatment or sandpaper treatment.

3.3. Air seal and recovery of HURT assembly

A similar percentage seal was obtained for both models of HURT assembly with no significant difference between each other ($p = 0.977$). This meant that the two models could be used interchangeably. Furthermore, good air seal of $> 92\%$ were obtained for both models to ensure that the HURT model assemblies were sealed sufficiently tight to be used in the study to determine particle deposition. On the other hand, the two HURT model assemblies had reasonable yield of $> 67\%$. Furthermore, the average percentage recoveries of the 2 HURT model

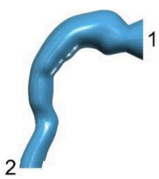
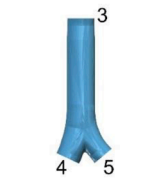
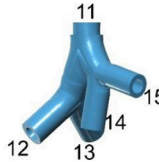
CAD Drawing	Actual Prints	Part	Length (mm)		Std Dev	Error	%Error
			CAD	Average			
		1	30.0	28.6	0.6	1.4	4.8
		2	16.0	14.7	0.3	1.3	8.3
		3	18.5	18.3	0.4	0.2	0.9
		4	17.2	17.3	0.5	0.1	0.4
		5	14.3	14.4	0.2	0.1	0.9
		6	15.0	13.4	0.5	1.6	10.7
		7	8.6	8.0	0.0	0.6	7.0
		8	8.1	7.3	0.2	0.8	9.9
		9	5.8	5.2	0.2	0.6	10.9
		10	9.6	9.4	0.3	0.2	2.4
		11	11.3	10.1	0.1	1.2	10.3
		12	8.1	7.8	0.3	0.3	3.3
		13	8.3	7.4	0.4	0.9	10.4
		14	8.0	7.6	0.2	0.4	4.6
		15	7.9	7.1	0.2	0.8	9.7

Fig. 3. Summary table for the various Dimensions of the CAD model VS actual printed model. All the dimensions are largely accurate and precise, with a percent error of less than 11%.

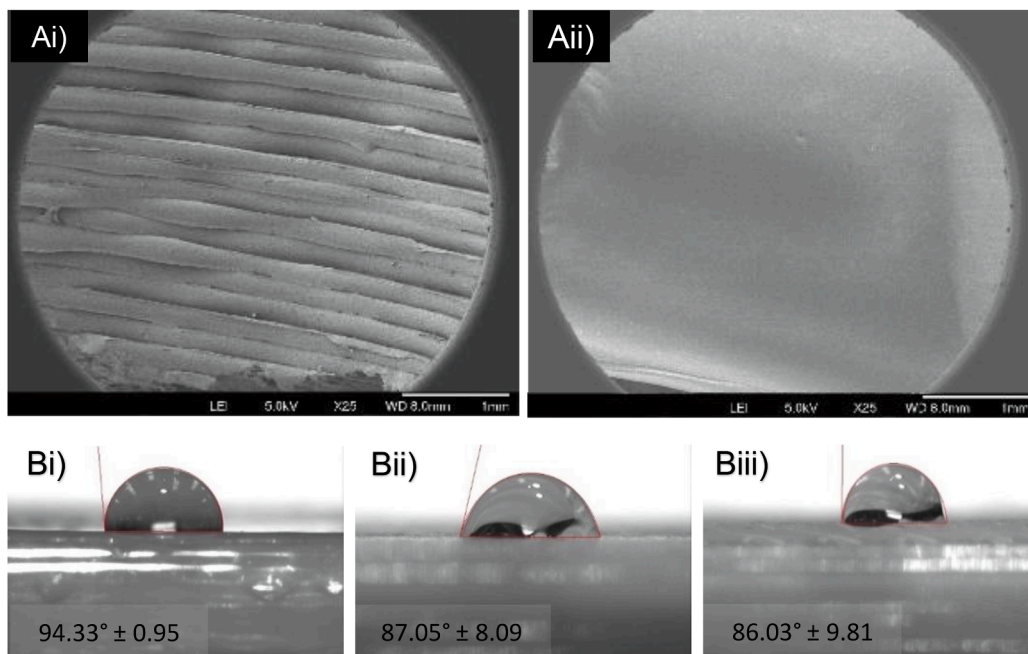


Fig. 4. Physical Characterization of 3D-printed Inhalation Testing Device. A) Effect of acetone treatment on the inner surface of 3D printed ABS lung model. Before treatment, visible layers were observed as illustrated in Ai). After treatment with acetone fumes, the inner surfaces become smooth with no visible lines between each layers of print as in Aii). Acetone vapour successfully smoothed out the gaps between each layer of prints. B) Water contact angle of various post treated surfaces. Bi) Acetone treated ABS, Bii) ABS smoothed with sandpaper, Biii) Untreated ABS. From the similar water contact angle, there is no significant effect of acetone treatment on the surface properties of ABS, in terms of hydrophobicity.

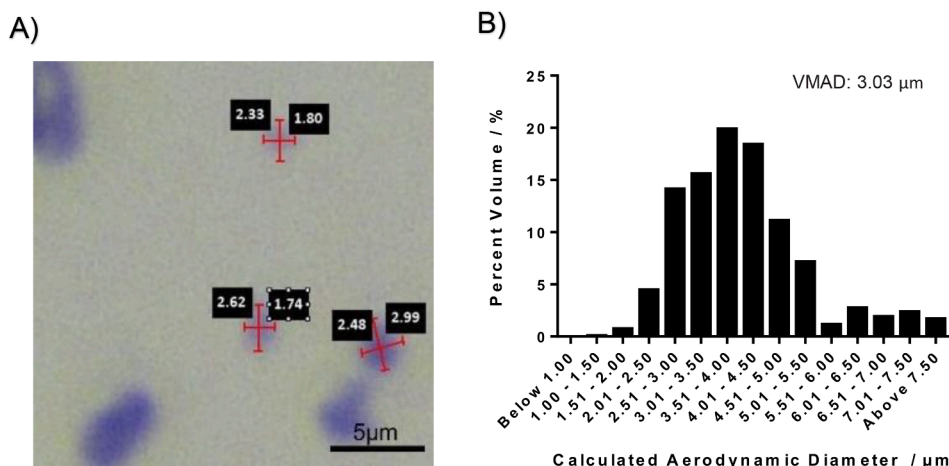


Fig. 5. Calculated Aerodynamic Diameter Distribution of Salbutamol Sulfate Particles. A) shows the size of salbutamol sulfate crystal being captured using a Nikon stereoscopic microscope coupled with NIS software. B) Calculated aerodynamic diameter distribution of salbutamol sulfate particle (808 particles).

assemblies were similar ($p = 0.753$) and could therefore be used interchangeably.

3.4. Evaluation of pMDI (Ventolin®)

Based on previous literature values, Ventolin® Evohaler has a mass median aerodynamic diameter (MMAD) of 2.28 µm (Terzano, 1999). Based on measurement of 808 microscopic images of sprayed on particles (Fig. 5) the calculated VMAD of a locally purchased Ventolin® Evohaler is 3.03 µm. VMAD is considered as the same value as MMAD, given a constant density of the inhaled particles. The calculated VMAD value and the MMAD value from the literature were comparable and can self-validate each other. Therefore, the VMAD value of 3.03 µm may be used for subsequent comparison with published *in vivo* radiological data.

3.5. Airway drug deposition study without spacer

Particle deposition study was conducted without the use of a spacer to determine the baseline deposition in the HURT model assembly (Fig. 6A). Regardless of airflow velocity, most particles deposited in the oropharyngeal region (63 – 86%), followed by the alveolar region (10 – 32%). Both tracheal (1 – 3%) and bronchial regions (1 – 3%) had significantly less particles deposited than the oropharyngeal and alveolar regions. As the airflow velocity was increased to simulate increasing physical activities, increasing percentage of inhaled particles deposited in the deeper region of the HURT model assembly, i.e., alveolar region. Percentage deposition in the alveolar region was 14.9% (15 LPM); 20.3% (25 LPM); 29% (35 LPM). In contrast, percentage deposition in the oropharyngeal region was 80.9% (15 LPM); 74.1% (25 LPM); 65.5% (35 LPM). Percentage deposition in the tracheal and bronchial regions remained similar regardless of airflow velocity.

3.6. Airway drug deposition study with spacer

Particle deposition study was repeated using all the same parameters, except for the additional use of spacer together with the HURT model assembly (Fig. 6B). Spacer is a commonly used device in the clinical setting, to prevent deposition of inhaled particle in the oropharyngeal region. Regardless of airflow velocity, the highest percentage of particles was deposited in the spacer (46 – 76%), followed by the alveolar region (17 – 46%). Contrastingly, the percentage of particles deposited in the oropharyngeal region (3 – 10%) is significantly less as compared to the results in the particle deposition study, without spacer. The remaining tracheal (0.7 – 2%) and bronchial regions (0.7 – 4%) had significantly less percentage of particles deposited, as

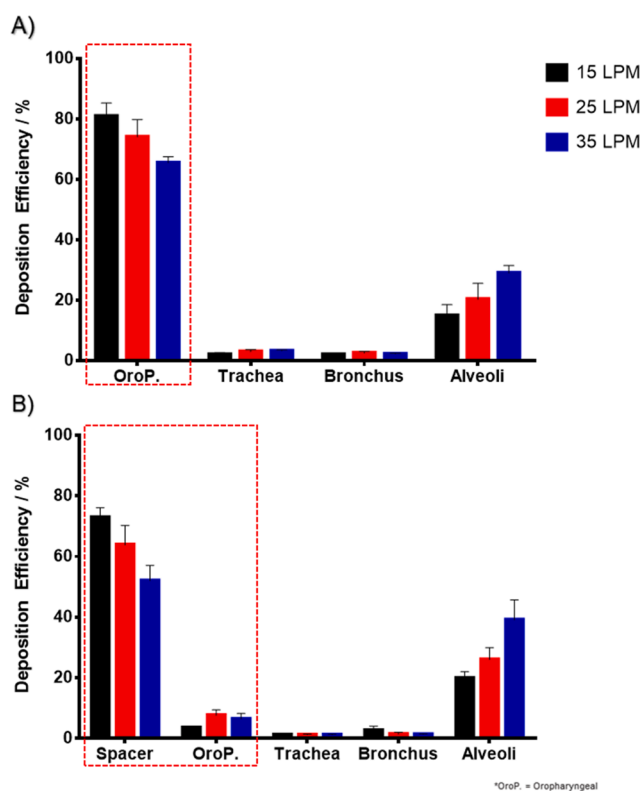


Fig. 6. Effect of Spacer on Particle Deposition at Various Parts of *In Vitro* HURT Model Assembly. Fig. 6A compares the % deposition of pMDI salbutamol in different parts of the HURT model assembly at 35 LPM, 25 LPM and 15 LPM without using a spacer. Fig. 6B compares the percentage deposition of salbutamol sulphate particles in different parts of the model at 35 LPM, 25 LPM and 15 LPM using a spacer. Without a spacer, up to 80% of drug particles were deposited in the oropharyngeal region, as reported in literature. Using a spacer, the deposition in oropharyngeal region is greatly reduced (65% to 6.4% at 35 LPM) and reflect greater similarity with *in vivo* deposition using nebulizer.

compared to the spacer and alveolar regions. A similar trend in particle deposition without a spacer was also observed. As the airflow velocity was increased to simulate increasing physical activities, increasing percentage of inhaled particles was deposited in the deeper region of the HURT model assembly, i.e., alveolar region. Percentage deposition at alveolar region was 19.8% (15 LPM); 26.0% (25 LPM); 39% (35 LPM).

Contrastingly, percentage deposition at spacer region was 72.9% (15 LPM); 63.8% (25 LPM); 52.0% (35 LPM). Percentage deposition in tracheal and bronchial regions remained similar regardless of airflow velocity.

4. Discussion

4.1. HURT model fabrication by 3D printing

In this study, we have demonstrated the use of a 3D printer to fabricate a HURT model, based on CT images of a healthy adult human male. The anatomically accurate model assembly was characterised and used in an *in vitro* particle deposition study with and without a spacer, to better simulate actual clinical settings of patients using pMDIs. The effect of different airflow through the model to simulate different respiratory minute volume of daily living was also investigated.

The 3D model designed was manufactured from acrylonitrile butadiene styrene (ABS) filament, a material commonly used in 3D printing (Garcia et al., 2018). To determine whether this model could address our aim, different designs were tested, and recovery studies were conducted. The model was initially designed using longer pipes but due to the formation of kinks, airflow was found to be disrupted. Instead, shorter pipes facilitated smooth airflow and thus these were used in the final model. Although there was an average of 68% recovery (Table 2), it can be assumed that retention is consistent throughout the whole model. Furthermore, the retained amount did not impact our study as we focused on the distribution of particles instead of percentage of absorption. To ensure that all particles were captured, the pass-through filter led into a solvent, capturing all remaining particles. Thus, it can be determined that the designed model was suitable for this study.

4.2. The use of a spacer as inhalation aid

As expected, without the use of any inhalation aid, such as a spacer, most of the inhaled drug particles deposited in the oropharyngeal region (Fig. 6). This is consistent with published literature data where ~80% of the inhaled particles deposited in the oropharyngeal region even with optimal inhalation technique while using a pMDI (Vincken et al., 2018). The pMDIs typically produce inhalation particles at a linear velocity (up to 25 kmh⁻¹), much faster than that of the airflow achieved by the patient during inhalation (up to 9 kmh⁻¹), resulting in the deposition at the back of the throat (Dalby et al., 2011). Furthermore, the sudden change in the direction of airflow (due to the geometry of the throat), may also have contributed to the deposition of particles by inertial impaction.

To reduce the deposition of particles in the oropharyngeal region, the very first concept of activating the pMDI into a spacer prior to inhalation was developed in the 1950 s (Stein and Thiel, 2017). The use of a spacer can significantly slow down the speed of aerosolised particles sprayed out from the pMDI, thus reducing the effect of inertial impaction and allowing enough time for the user to inhale the particles. This often

Table 2

Seal and Recovery Test for the 2 Replicates of HURT Model Assemblies. The consistent percentage seal and percentage recovery between the two replicates models illustrates that the 3D printed models are replicable and can be used interchangeably.

A) Seal Test		
	Average /%	SD
Model A	92.4	0.8
Model B	92.4	1.6
B) Recovery Test		
	Average /%	SD
Model A	69.0	6.0
Model B	67.3	8.0

results in a significant reduction in oropharyngeal deposition of inhaled particles (Vincken et al., 2018). A similar trend was observed in the HURT model assembly where the use of a spacer. This demonstrated the similarity of the HURT model assembly to actual human *in vivo* setting for inhalation particle deposition, with or without the use of spacer.

4.3. Effect of airflow velocity on particle deposition

To further demonstrate the *in vitro-in vivo* correlation of the HURT model assembly, the effect of airflow velocity was also investigated in this study. Although resting human flow rate is between 7 and 8 LPM, greater effort is required when using an MDI. Thus, the airflow velocity of 15 LPM was chosen and the velocities 25 and 35 LPM were determined based on the British Pharmacopoeia (BP) recommendation of 30 L/min (± 5 per cent) for pressurized inhalers in the *in vitro* studies (BP Appendix XII C). Particle diameters between 3 and 4 μ m are used in commercial dose inhalers, thus the deposition of particle size 3.1 μ m was investigated. As expected, an increase in the airflow velocity resulted in a higher deposition of particles in the lower airways region or the alveolar region. This trend is similar to those reported in bicycle messengers and their exposure to pollution. With a significantly higher pulmonary ventilation, bicycle messengers have an estimated 4-fold more exposure to the amount of polluted air inhaled (Bernmark et al., 2006). In a separate study by Daige et al. (2003), it was demonstrated that the total number of deposited ultra-fine particles, although much smaller than in our study at a median of 26 nm, was 4.5-fold higher during exercise than during rest due to a combination of factors such as an increase in deposited fraction, increase in intake of particles and the shifting of deposition towards the alveolar region (Daige et al., 2003).

4.4. Compare HURT testing with human study

In vivo human data using radio-labelled monodispersed particles had been performed previously (Fleming et al., 2015; Majoral et al., 2014). The *in vivo* data used for comparison in this case were that of a 3.1 μ m ADD radio-labelled monodispersing droplets administered through a vibrating mesh nebuliser (Fleming et al., 2015; Majoral et al., 2014), to healthy human adults at the resting state. The radiopharmaceutical aerosol consisted of nebulized aqueous droplets produced from a suspension of Tc-99 m labelled milli-microspheres of human serum albumin in isotonic saline (0.9 %w/v sodium chloride). In Fig. 7, *in vitro* deposition data using the HURT model assembly at 15 LPM, with spacer, were compared against the published *in vivo* human deposition data due

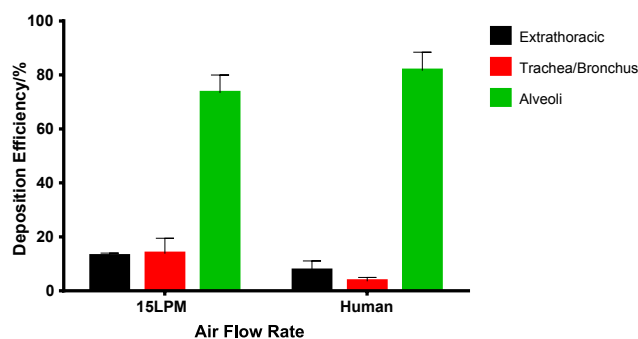


Fig. 7. Particle Deposition for *In Vitro* HURT Model Assembly vs. Radioactive Aerosol Deposition Human Data. Fig. 7 compares the % deposition of pMDI salbutamol sulphate particles measured by our *in vitro* HURT model assembly at 15 LPM using a spacer (Aerochamber®), with actual human data based on a nebuliser deposition of a monodispersion of 3.1 μ m aerodynamic diameter droplets (Fleming et al., 2015). The pattern of deposition across different regions of the lungs (extrathoracic, trachea/bronchus and alveoli) are similar with alveoli having the highest deposition, and trachea/bronchus having the lowest deposition. There are no significant differences for all 3 regions of the lung model assembly and human data.

to it being closest to that of the minute respiratory volume of healthy human adults at resting state (average of 8.3 LPM) (Fleming et al., 2015). In all three regions of extrathoracic, tracheobronchial and alveolar region, there was no significant difference between the deposition in the *in vitro* HURT model assembly with spacer and the *in vivo* human data (p-value of 0.057, 0.082, 0.170 respectively). In both cases, the highest percentage of deposited particles were in the alveolar region (73.3% vs 81.6%), which was the most important site of deposition in the HURT.

Besides, Ammari et al., evaluated the lung and systemic bioavailability of salbutamol post-inhalation from a Ventolin Evohaler, either with or without an ABLER Spacer™ (Ammari et al., 2020; Mazhar and Chrystyn, 2008). In the published study, 16 healthy adults inhaled two puffs of 100 µg salbutamol with a peak inhalation flow between 30 and 60 L/min. In Fig. 8, *in vitro* deposition data using a Ventolin Evohaler with and without an Aerochamber with the HRT model assembly at 35 LPM was compared with the published *in vivo* data of salbutamol inhalation using a Ventolin Evohaler, with and without the use of an ABLER Spacer™. Whilst the *in vitro* extrathoracic region data was compared with the *in vivo* oropharyngeal deposition data, the total *in vitro* deposition in trachea, bronchus and alveoli was compared with the *in vivo* urinary recovery of unchanged salbutamol 0–0.5 h (USALO.5) post-salbutamol inhalation. Ammari et al., 2020 defined USALO.5 as the relative lung bioavailability of inhaled salbutamol. The relative lung bioavailability represents the total amount of salbutamol deposited in the lungs, specifically the trachea, bronchus and alveoli. Thus, total deposition in trachea, bronchus and alveoli *in vitro* was compared to the *in vivo* USALO.5 data.

Both *in vitro* and *in vivo* data illustrated that there was greater particle deposition in the extrathoracic region than the trachea, bronchus and alveoli region when a spacer was not used (Fig. 8A). On the other hand, both *in vitro* and *in vivo* data exhibited greater particle deposition in the trachea, bronchus, and alveoli region in comparison to the extrathoracic region with the use of a spacer (Fig. 8B). The slight difference in extrathoracic deposition could be due to the difference in the spacers used in the *in vitro* testing and human study, i.e., the Aerochamber® mouthpiece vs the ABLER Spacer™ mouthpiece. A study conducted by Nicola et al., determined that fewer particles were deposited within the Aerochamber® mouthpiece compared to an ABLER Spacer™ mouthpiece, meaning that greater number of particles are able to exit the Aerochamber® mouthpiece and enter the extrathoracic region instead

(Nicola et al., 2020).

4.5. Inhalation drug testing methods

Historically, the most common approach of administration is via a small-volume nebuliser (SVN). Current gold standard for *in vivo* radiological study is to use an SVN to generate and administer the drug aerosol particles. This was also the case for the set of *in vivo* human data used for comparison in this study. Only 15 LPM was investigated *in vivo* as there is no other existing *in vivo* data to draw comparisons to, due to difficulty in having patients run and breath into an inhaler simultaneously. Several reviews of *in vivo* clinical studies demonstrated that pMDI with a spacer is as effective as SVN (Al-Sallami Hesham et al., 2001; Cates et al., 2013; Salyer et al., 2008; van Geffen et al., 2016). Based on similar efficacy, it was assumed that both the use of pMDI with spacer and the use of SVN are similar in their particle deposition profile in the respiratory tract.

Current *in vitro* standard in quality control testing for inhalation drug devices include the use of cascade impactors such as Andersen Cascade Impactor or Next Generation Impactor (NGI). A comparison between our model and existing models, such as NGIs, was not conducted as these two models have different purposes. NGIs are solely utilised to perform quality control tests on particle retention whereas our model was designed to mimic *in vivo* data and provide a future alternative method to human clinical trials. While existing models are useful for standardising and controlling the quality of inhalation products, they are not able to perfectly simulate the respiratory tract, since they operate at a constant flow rate, while the respiratory cycle has a varying flow-time profile (Mitchell et al., 2007). To better simulate the actual *in vivo* environment using *in vitro* devices, the most common approach is to design a device that best resemble the HURT (Byron et al., 2010). This was evident in the case of the Alberta Idealised Throat model or the use of various dimensions of mouth throat model for airway drug deposition study (Wei et al., 2018). Carrigy et al. also used CT scanned images of paediatric populations to create a realistic extrathoracic model for particle deposition study (Carrigy et al., 2014).

Although the extrathoracic region has been suggested to be the major source of variability in airway deposition of inhaled drugs (Byron et al., 2010), additional airway replica down to the bronchus may potentially provide a more accurate *in vitro-in vivo* correlation due to the close relationship between airway geometry and airflow velocity (Rahimi-

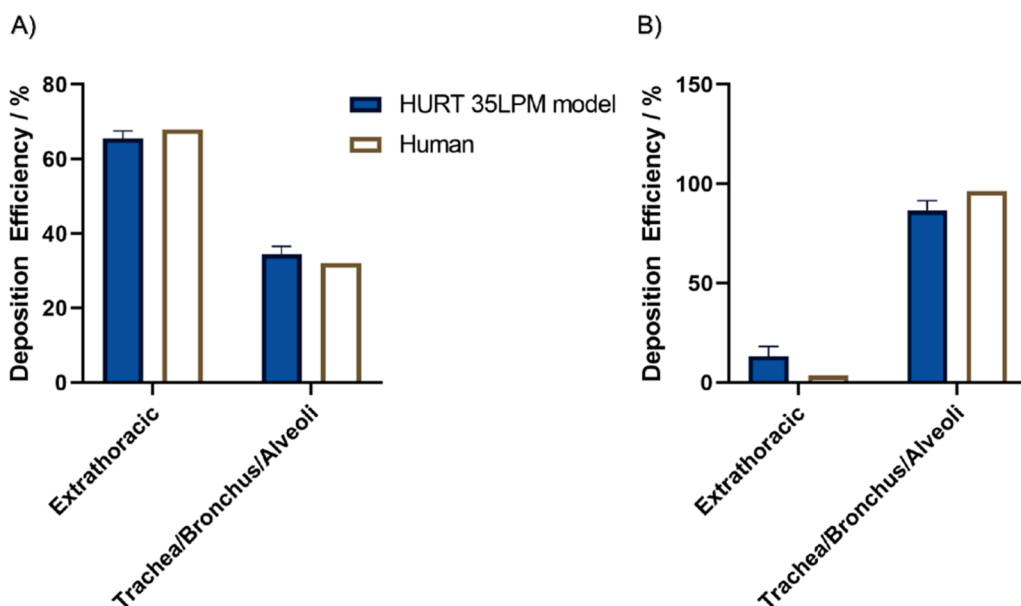


Fig. 8. Particle Deposition data from *In Vitro* HURT Model Assembly vs. Human Study, using Ventolin Evohaler. Fig. 8 compares the % deposition of salbutamol sulphate particles measured by our *in vitro* HURT model at 35 LPM, with actual human data, at 30–60 LPM (Ammari et al., 2020). A) Comparison of our *in vitro* salbutamol sulphate deposition data without a spacer to *in vivo* salbutamol deposition data without a spacer. B) Comparison of our *in vitro* salbutamol sulphate deposition data with an Aerochamber® spacer with human salbutamol deposition data with an ABLER Spacer™. There was greater particle deposition in the trachea, bronchus and alveoli than the extrathoracic region when using a spacer. Without a spacer there was greater particle deposition in the extrathoracic region than the trachea, bronchus, and alveoli region. Errors bars were omitted for the human data as individual values were not obtainable from the study.

Gojri et al., 2016). Other research groups have focused on creating a chemical environment that resembles that of the HURT, such as lining the *in vitro* device with polythene oxide solution that act as a mucus simulant (Kim and Eldridge, 1985). However, the coating of the HURT with these mucus simulants can be difficult.

In consideration of the current developments of *in vitro* devices for aerosol testing, our 3D printed HURT model assembly is foreseen to provide several advantages for future airway drug deposition testing. Firstly, the ability to incorporate human CT scan images for 3D printing means that personalisation of testing devices may now be possible. Users may potentially have a more accurate testing device before they start to use the product. Secondly, as most clinical trials do not include geriatric and paediatric subjects, the results from these trials are at best extrapolated to usage in these special populations. With a personalised airway drug deposition testing device, it may be potentially possible to predict the particle deposition in geriatric and paediatric patients. Thirdly, CT scanned images of users with respiratory diseases such as COPD or cystic fibrosis can also be used. In COPD, airways are narrower and filled with scar tissues. With deposition data of these subgroups of patients potentially available, pharmacotherapy can then be personalized and optimized (Chung, 2005). Finally, although this model is based off one patient, the whole system has significant potential in the personalised medicine field, such as being employed as an airway drug deposition study device to determine the degree of deposition in the HURT at various pollution level, thereby predicting any potential health outcomes due to pollution levels in the environment.

4.6. Limitations of this study

A few limitations of the current study are as follows. We tested only Ventolin®, which is a relatively simple pMDI formulation with salbutamol sulphate suspended in the propellant, 1, 1, 1, 2-tetrafluoroethane. Other pMDIs with different formulations should also be tested for *in vitro-in vivo* correlation, especially since it is well known that the formulation can affect drug deposition profile within the respiratory tract (Schroeter et al., 2018). Other than pMDIs, inhalation devices such as DPIs or nebulizers with varying aerodynamic sizes should also be tested. This model also did not mimic lung physiological conditions such as throat temperature and mucus layer. In the future, this model may be improved by adding a surfactant along the inner walls to mimic the human mucus layer. Another way to mimic thermal physiological conditions is by embedding water capillaries into the walls (Asgari et al., 2019).

In addition, the current design of the HURT model assembly was tested at a constant airflow rate. However, our human respiratory cycle had a varying airflow profile. To address this limitation, future studies can utilise a breathing simulator instead to better replicate human breathing patterns. It is recommended that future studies also measure exhalation airflow as this parameter was also excluded in the current study. Furthermore, measuring the length to determine error in production is a technical limitation of this study. Instead, determining error based on diameter may be more appropriate for this study as a difference in diameter could influence particle deposition. Finally, the print accuracy of the HURT model was ~ 90%. A 3D printer with higher resolution may be used in the future to allow a more accurate HURT model assembly to be fabricated.

5. Conclusion

A morphologically accurate adult human HURT assembly using an FDM printer with thermoplastic ABS for airway deposition study was fabricated. With an accurate morphology of adult HURT and the use of a spacer, we demonstrated a similar deposition pattern compared to *in vivo* human data. This creation of an *in vitro* physical device modelled after an adult HURT may provide a good *in vitro-in vivo* airway deposition correlation and provide opportunities for personalized deposition

studies in special populations or disease states.

Funding

Singapore National Additive Manufacturing Innovation Cluster (NAMIC) project 2,016,011 and an MOE AcRF Tier 1 grant (R148-000-224-112).

CRediT authorship contribution statement

Seng Han Lim: Writing - original draft, Visualization, Data curation, Investigation, Methodology. **Sol Park:** Writing - original draft, Visualization, Data curation, Investigation. **Chun Chuan Lee:** Writing - original draft, Visualization, Data curation, Investigation. **Paul Chi Lui Ho:** Writing - review & editing, Supervision. **Philip Chi Lip Kwok:** Writing - review & editing, Methodology, Validation. **Lifeng Kang:** Funding acquisition, Supervision, Writing - review & editing, Conceptualization.

Declaration of Competing Interest

The authors declare that they have no known competing financial interests or personal relationships that could have appeared to influence the work reported in this paper.

References

- Al-Sallami Hesham, S., Ball Patrick, A., Davey Andrew, K., 2001. Metered-dose inhaler with spacer versus nebuliser for acute exacerbation of asthma—a literature review. *Aust. J. Hosp. Pharm.* 31, 189–192. <https://doi.org/10.1002/jppr2001313189>.
- Ammari, W.G., Oriquat, G.A., Sanders, M., 2020. Comparative pharmacokinetics of salbutamol inhaled from a pressurized metered dose inhaler either alone or connected to a newly enhanced spacer design. *Eur. J. Pharm. Sci.* 147, 105304 <https://doi.org/10.1016/j.ejps.2020.105304>.
- Asgari, M., Lucci, F., Bialek, J., Dunan, B., Andreatta, G., Smajda, R., Lani, S., Blondiaux, N., Majeed, S., Steiner, S., Schaller, J.-P., Frenzel, S., Hoeng, J., Kuczaj, A.K., 2019. Development of a realistic human respiratory tract cast representing physiological thermal conditions. *Aerosol Sci. Technol.* 53, 860–870. <https://doi.org/10.1080/02786826.2019.1612839>.
- Bernmark, E., Wiktorin, C., Svartengren, M., Lewné, M., Åberg, S., 2006. Bicycle messengers: energy expenditure and exposure to air pollution. *Ergonomics* 49, 1486–1495. <https://doi.org/10.1080/00140130600708206>.
- Brand, P., Hederer, B., Austen, G., Dewberry, H., Meyer, T., 2008. Higher lung deposition with respimat soft mist inhaler than HFA-MDI in COPD patients with poor technique. *Int. J. Chron. Obstruct. Pulmon. Dis.* 3, 763–770. <https://doi.org/10.2147/COPD.S3930>.
- Byron, P.R., Hindle, M., Lange, C.F., Longest, P.W., McRobbie, D., Oldham, M.J., Olsson, B., Thiel, C.G., Wachtel, H., Finlay, W.H., 2010. In vivo-in vitro correlations: predicting pulmonary drug deposition from pharmaceutical aerosols. *J. Aerosol Med. Pulm. Drug Deliv.* 23 (Suppl 2), S59–S69. <https://doi.org/10.1089/jamp.2010.0846>.
- Carrigy, N.B., Ruzyczki, C.A., Golshahi, L., Finlay, W.H., 2014. Pediatric in vitro and in silico models of deposition via oral and nasal inhalation. *J. Aerosol Med. Pulm. Drug Deliv.* 27, 149–169. <https://doi.org/10.1089/jamp.2013.1075>.
- Cates, C.J., Welsh, E.J., Rowe, B.H., 2013. Holding chambers (spacers) versus nebulisers for beta-agonist treatment of acute asthma. *Cochrane Database Syst. Rev.*, Cd000052. <https://doi.org/10.1002/14651858.CD000052.pub3>.
- Chen, G., Y., X., Kwok, C.H.P., Kang, L., 2020. Pharmaceutical applications of 3D printing. *Addit. Manuf.* 34, 1012094. <https://doi.org/10.1016/j.addma.2020.101209>.
- Cheng, K.H., Cheng, Y.S., Yeh, H.C., Swift, D.L., 1997. Measurements of airway dimensions and calculation of mass transfer characteristics of the human oral passage. *J. Biomech. Eng.* 119, 476–482. <https://doi.org/10.1115/1.2798296>.
- Chiou, H., Li, L., Hu, T., Chan, H.K., Chen, J.F., Yun, J., 2007. Production of salbutamol sulfate for inhalation by high-gravity controlled antisolvent precipitation. *Int. J. Pharm.* 331, 93–98. <https://doi.org/10.1016/j.ijpharm.2006.09.022>.
- Chow, A.H., Tong, H.H., Chattopadhyay, P., Shekunov, B.Y., 2007. Particle engineering for pulmonary drug delivery. *Pharm. Res.* 24, 411–437. <https://doi.org/10.1007/s11095-006-9174-3>.
- Chung, K.F., 2005. The role of airway smooth muscle in the pathogenesis of airway wall remodeling in chronic obstructive pulmonary disease. *Proc. Am. Thorac. Soc.* 2, 347–354. <https://doi.org/10.1513/pats.200504-028SR>.
- Daigle, C.C., Chalupa, D.C., Gibb, F.R., Morrow, P.E., Oberdörster, G., Utell, M.J., Frampton, M.W., 2003. Ultrafine particle deposition in humans during rest and exercise. *Inhal. Toxicol.* 15, 539–552. <https://doi.org/10.1080/089583703044468>.
- Dalby, R.N., Eicher, J., Zierenberg, B., 2011. Development of respimat(R) soft mist inhaler and its clinical utility in respiratory disorders. *Med. Devices* 4, 145–155. <https://doi.org/10.2147/mder.s7409>.

- Delvadia, R.R., Longest, P.W., Byron, P.R., 2012. In vitro tests for aerosol deposition. I: scaling a physical model of the upper airways to predict drug deposition variation in normal humans. *J. Aerosol Med. Pulm. Drug Deliv.* 25, 32–40. <https://doi.org/10.1089/jamp.2011.0905>.
- EMA, accessed 18/01/2021. Guideline on the pharmaceutical quality of inhalation and nasal products. http://www.ema.europa.eu/docs/en_GB/document_library/Scientific_guideline/2009/09/WC500003568.pdf.
- Fehr, A.R., Perlman, S., 2015. Coronaviruses: an overview of their replication and pathogenesis. *Methods Mol. Biol.* 1282, 1–23. https://doi.org/10.1007/978-1-4939-2438-7_1.
- Feng, Y., Zhao, J., Chen, X., Lin, J., 2017. An in silico subject-variability study of upper airway morphological influence on the airflow regime in a tracheobronchial tree. *Bioeng. (Basel, Switzerland)* 4. <https://doi.org/10.3390/bioengineering4040090>.
- Fernandez Tena, A., Casan Clara, P., 2012. Deposition of inhaled particles in the lungs. *Arch. Bronconeumol.* 48, 240–246. <https://doi.org/10.1016/j.arbres.2012.02.003>.
- Fleming, J., Conway, J., Majoral, C., Katz, I., Caillibotte, G., Pichelin, M., Montesantos, S., Bennett, M., 2015. Controlled, parametric, individualized, 2-D and 3-D imaging measurements of aerosol deposition in the respiratory tract of asthmatic human subjects for model validation. *J. Aerosol Med. Pulm. Drug Deliv.* 28, 432–451. <https://doi.org/10.1089/jamp.2014.1191>.
- Gandhimathi, C., Venugopal, J.R., Sundararajan, S., Sridhar, R., Tay, S.S., Ramakrishna, S., Kumar, S.D., 2015. Breathable medicine: pulmonary mode of drug delivery. *J. Nanosci. Nanotechnol.* 15, 2591–2604. <https://doi.org/10.1166/jnn.2015.10341>.
- Garcia, J., Yang, Z., Mongrain, R., Leask, R.L., Lachapelle, K., 2018. 3D printing materials and their use in medical education: a review of current technology and trends for the future. *BMJ Simul. Technol. Enhanc. Learn.* 4, 27–40. <https://doi.org/10.1136/bmjstel-2017-000234>.
- Goole, J., Amighi, K., 2016. 3D printing in pharmaceuticals: a new tool for designing customized drug delivery systems. *Int. J. Pharm.* 499, 376–394. <https://doi.org/10.1016/j.ijpharm.2015.12.071>.
- Greenblatt, E.E., Winkler, T., Harris, R.S., Kelly, V.J., Kone, M., Katz, I., Martin, A.R., Caillibotte, G., Venegas, J., 2015. What causes uneven aerosol deposition in the bronchoconstricted lung? A quantitative imaging study. *J. Aerosol Med. Pulm. Drug Deliv.* 28, 57–75. <https://doi.org/10.1089/jamp.2014.1197>.
- Guo, C., Gillespie, S.R., Kauffman, J., Doub, W.H., 2008. Comparison of delivery characteristics from a combination metered-dose inhaler using the Andersen cascade impactor and the next generation pharmaceutical impactor. *J. Pharm. Sci.* 97, 3321–3334. <https://doi.org/10.1002/jps.21203>.
- Hess, D.R., 2008. Aerosol delivery devices in the treatment of asthma. *Respir. Care* 53, 699–723. <https://pubmed.ncbi.nlm.nih.gov/18501026/>.
- Heyder, J., Gebhart, J., Rudolf, G., Schiller, C.F., Stahlhofen, W., 1986. Deposition of particles in the human respiratory tract in the size range 0.005–15 µm. *J. Aerosol Sci.* 17, 811–825. [https://doi.org/10.1016/0021-8502\(86\)90035-2](https://doi.org/10.1016/0021-8502(86)90035-2).
- Ibrahim, M., Verma, R., Garcia-Contreras, L., 2015. Inhalation drug delivery devices: technology update. *Med. Devices* 8, 131–139. <https://doi.org/10.2147/mdir.s48888>.
- Katz, I.M., Schroeter, J.D., Martonen, T.B., 2001. Factors affecting the deposition of aerosolized insulin. *Diabetes Technol. Ther.* 3, 387–397. <https://doi.org/10.1089/15209150152607169>.
- Kim, C.S., Eldridge, M.A., 1985. Aerosol deposition in the airway model with excessive mucous secretions. *J. Appl. Physiol.* 59, 1766–1772. <https://doi.org/10.1152/jappl.1985.59.6.1766>.
- Kim, G.B., Lee, S., Kim, H., Yang, D.H., Kim, Y.H., Kyung, Y.S., Kim, C.S., Choi, S.H., Kim, B.J., Ha, H., Kwon, S.U., Kim, N., 2016. Three-dimensional printing: basic principles and applications in medicine and radiology. *Korean J. Radiol.* 17, 182–197. <https://doi.org/10.3348/kjr.2016.17.2.182>.
- Kim, S.Y., Wong, A.H., Abou Neel, E.A., Chrzanoski, W., Chan, H.K., 2015. The future perspectives of natural materials for pulmonary drug delivery and lung tissue engineering. *Expert. Opin. Drug Deliv.* 12, 869–887. <https://doi.org/10.1517/17425247.2015.993314>.
- Koleva, E.L., Feng, Y., Fromen, C.A., 2020. Realizing lobe-specific aerosol targeting in a 3D-printed in vitro lung model. *J. Aerosol Med. Pulm. Drug Deliv.* <https://doi.org/10.1089/jamp.2019.1564>.
- Labiris, N.R., Dolovich, M.B., 2003a. Pulmonary drug delivery. Part I: physiological factors affecting therapeutic effectiveness of aerosolized medications. *Br. J. Clin. Pharmacol.* 56, 588–599. <https://www.ncbi.nlm.nih.gov/pubmed/14616418>.
- Labiris, N.R., Dolovich, M.B., 2003b. Pulmonary drug delivery. Part II: the role of inhaler delivery devices and drug formulations in therapeutic effectiveness of aerosolized medications. *Br. J. Clin. Pharmacol.* 56, 600–612. <https://doi.org/10.1046/j.1365-2125.2003.01893.x>.
- Laube, B.L., Janssens, H.M., de Jongh, F.H., Devadason, S.G., Dhand, R., Diot, P., Everard, M.L., Horvath, I., Navalesi, P., Voshaar, T., Chrystyn, H., 2011. What the pulmonary specialist should know about the new inhalation therapies. *Eur. Respir. J.* 37, 1308–1331. <https://doi.org/10.1183/09031936.00166410>.
- Lewis, D.A., O'Shea, H., Church, T.K., Brambilla, G., Traini, D., Young, P.M., 2016. Exploring the impact of sample flowrate on in vitro measurements of metered dose inhaler performance. *Int. J. Pharm.* 514, 420–427. <https://doi.org/10.1016/j.ijpharm.2016.05.025>.
- Liang, Z., Ni, R., Zhou, J., Mao, S., 2015. Recent advances in controlled pulmonary drug delivery. *Drug Discov. Today* 20, 380–389. <https://doi.org/10.1016/j.drudis.2014.09.020>.
- Lim, S.H., Kathuria, H., Tan, J.J.Y., Kang, L., 2018. 3D printed drug delivery and testing systems - a passing fad or the future? *Adv. Drug Deliv. Rev.* 139–168. <https://doi.org/10.1016/j.addr.2018.05.006>.
- Liu, W., Li, Y., Liu, J., Niu, X., Wang, Y., Li, D., 2013. Application and performance of 3D printing in nanobiomaterials. *J. Nanomater.* 2013, 7. <https://doi.org/10.1155/2013/681050>.
- Majoral, C., Fleming, J., Conway, J., Katz, I., Tossici-Bolt, L., Pichelin, M., Montesantos, S., Caillibotte, G., 2014. Controlled, parametric, individualized, 2D and 3D imaging measurements of aerosol deposition in the respiratory tract of healthy human volunteers: in vivo data analysis. *J. Aerosol Med. Pulm. Drug Deliv.* 27, 349–362. <https://doi.org/10.1089/jamp.2013.1065>.
- Mazhar, S.H.R.A., Chrystyn, H., 2008. Salbutamol relative lung and systemic bioavailability of large and small spacers. *J. Pharm. Pharmacol.* 60, 1609–1613. <https://doi.org/10.1211/jpp.60.12.0006>.
- Mitchell, J., Newman, S., Chan, H.-K., 2007. In vitro and in vivo aspects of cascade impactor tests and inhaler performance: a review. *AAPS PharmSciTech* 8, 237–248. <https://doi.org/10.1208/pt0804110>.
- Nicola, M., Soliman, Y.M.A., Hussein, R., Saeed, H., Abdelrahim, M., 2020. Comparison between traditional and nontraditional add-on devices used with pressurized metered-dose inhalers. *ERJ Open Res.* 6, 00073–02020. <https://openres.ersjournals.com/content/6/4/00073-2020>.
- Oakes, J.M., Breen, E.C., Scadeng, M., Tchanchou, G.S., Darquenne, C., 2014. MRI-based measurements of aerosol deposition in the lung of healthy and elastase-treated rats. *J. Appl. Physiol.* 116, 1561–1568. <https://doi.org/10.1152/jappphysiol.01165.2013>.
- Rahimi-Gorji, M., Gorji, T.B., Gorji-Bandpy, M., 2016. Details of regional particle deposition and airflow structures in a realistic model of human tracheobronchial airways: two-phase flow simulation. *Comput. Biol. Med.* 74, 1–17. <https://doi.org/10.1016/j.combiomed.2016.04.017>.
- RDDOnline, accessed 18/01/2021. Respiratory drug delivery online. <https://www.rddonline.com/>.
- Ruigrok, M.J.R., Frijlink, H.W., Hinrichs, W.L.J., 2016. Pulmonary administration of small interfering RNA: The route to go? *J. Control. Release* 235, 14–23. <https://doi.org/10.1016/j.jconrel.2016.05.054>.
- Sa, R.C., Zeman, K.L., Bennett, W.D., Prisk, G.K., Darquenne, C., 2015. Effect of posture on regional deposition of coarse particles in the healthy human lung. *J. Aerosol Med. Pulm. Drug Deliv.* 28, 423–431. <https://doi.org/10.1089/jamp.2014.1189>.
- Salyer, J.W., DiBlasi, R.M., Crotwell, D.N., Cowan, C.A., Carter, E.R., 2008. The conversion to metered-dose inhaler with valved holding chamber to administer inhaled albuterol: a pediatric hospital experience. *Respir. Care* 53, 338–345. <https://pubmed.ncbi.nlm.nih.gov/18291050/>.
- Schroeter, J.D., Sheth, P., Hickey, A.J., Asgharian, B., Price, O.T., Holt, J.T., Conti, D.S., Saluja, B., 2018. Effects of formulation variables on lung dosimetry of albuterol sulfate suspension and beclomethasone dipropionate solution metered dose inhalers. *AAPS PharmSciTech* 19, 2335–2345. <https://doi.org/10.1208/s12249-018-1071-7>.
- Segal, R.A., Martonen, T.B., Kim, C.S., 2000. Comparison of computer simulations of total lung deposition to human subject data in healthy test subjects. *J. Air Waste Manag. Assoc.* 50, 1262–1268. <https://doi.org/10.1080/10473289.2000.10464155>.
- Stein, S.W., Thiel, C.G., 2017. The history of therapeutic aerosols: a chronological review. *J. Aerosol Med. Pulm. Drug Deliv.* 30, 20–41. <https://doi.org/10.1089/jamp.2016.1297>.
- Stuart, B.O., 1976. Deposition and clearance of inhaled particles. *Environ. Health Perspect.* 16, 41–53. <https://doi.org/10.1289/ehp.761641>.
- Sturm, R., 2016. Bioaerosols in the lungs of subjects with different ages-part 1: deposition modeling. *Ann. Transl. Med.* 4, 211. <https://doi.org/10.21037/atm.2016.05.62>.
- Taber, R., Rafee, R., Valipour, M.S., Ahmadi, G., 2020. Investigation of airflow at different activity conditions in a realistic model of human upper respiratory tract. *Comput. Methods Biomech. Biomed. Eng.* 1–15. <https://doi.org/10.1080/10255842.2020.1819256>.
- Taki, M., Marriott, C., Zeng, X.M., Martin, G.P., 2010. Aerodynamic deposition of combination dry powder inhaler formulations in vitro: a comparison of three impactors. *Int. J. Pharm.* 388, 40–51. <https://doi.org/10.1016/j.ijpharm.2009.12.031>.
- Terzano, C., 1999. Metered dose inhalers and spacer devices. *Eur. Rev. Med. Pharmacol. Sci.* 3, 159–169. <https://www.europeanreview.org/wp/wp-content/uploads/240.pdf>.
- Thompson, R.B., Finlay, W.H., 2012. Using MRI to measure aerosol deposition. *J. Aerosol Med. Pulm. Drug Deliv.* 25, 55–62. <https://doi.org/10.1089/jamp.2011.0897>.
- Tian, G., Longest, P.W., Su, G., Hindle, M., 2011a. Characterization of respiratory drug delivery with enhanced condensational growth using an individual path model of the entire tracheobronchial airways. *Ann. Biomed. Eng.* 39, 1136–1153. <https://doi.org/10.1007/s10439-010-0223-z>.
- Tian, G., Longest, P.W., Su, G., Walenga, R.L., Hindle, M., 2011b. Development of a stochastic individual path (SIP) model for predicting the tracheobronchial deposition of pharmaceutical aerosols: effects of transient inhalation and sampling the airways. *J. Aerosol Sci.* 42, 781–799. <https://doi.org/10.1016/j.jaerosci.2011.07.005>.
- van Geffen, W.H., Douma, W.R., Slebos, D.J., Kerstjens, H.A., 2016. Bronchodilators delivered by nebuliser versus pMDI with spacer or DPI for exacerbations of COPD. *Cochrane Database Syst. Rev.*, Cd011826. <https://doi.org/10.1002/14651858.CD011826.pub2>.
- Vincken, W., Levy, M.L., Scullion, J., Usmani, O.S., Dekhuijzen, P.N.R., Corrigan, C.J., 2018. Spacer devices for inhaled therapy: why use them, and how? *ERJ Open Res.* 4, 00065–02018. <https://doi.org/10.1183/23120541.00065-2018>.
- Wei, X., Hindle, M., Kaviratna, A., Huynh, B.K., Delvadia, R.R., Sandell, D., Byron, P.R., 2018. In vitro tests for aerosol deposition. VI: realistic testing with different mouth-throat models and in vitro-in vivo correlations for a dry powder inhaler, metered dose inhaler, and soft mist inhaler. *J. Aerosol Med. Pulm. Drug Deliv.* 358–371. <https://doi.org/10.1089/jamp.2018.1454>.

- Wikimedia, accessed 18/01/2021. Illu conducting passages.svg. Wikimedia Commons. https://commons.wikimedia.org/w/index.php?title=File:Illu_conducting_passages.svg&oldid=292678937.
- Xi, J., Longest, P.W., 2007. Transport and deposition of micro-aerosols in realistic and simplified models of the oral airway. *Ann. Biomed. Eng.* 35, 560–581. <https://doi.org/10.1007/s10439-006-9245-y>.
- Xi, J., Longest, P.W., 2008. Effects of oral airway geometry characteristics on the diffusional deposition of inhaled nanoparticles. *J. Biomech. Eng.* 130, 011008 <https://doi.org/10.1115/1.2838039>.
- Xi, J., Yang, T., Talaat, K., Wen, T., Zhang, Y., Klozik, S., Peters, S., 2018. Visualization of local deposition of nebulized aerosols in a human upper respiratory tract model. *J. Vis.* 21, 225–237. <https://doi.org/10.1007/s12650-017-0456-0>.
- Yang, M.Y., Chan, J.G., Chan, H.K., 2014. Pulmonary drug delivery by powder aerosols. *J. Control. Release* 193, 228–240. <https://doi.org/10.1016/j.jconrel.2014.04.055>.
- Yeh, H.C., Schum, G.M., 1980. Models of human lung airways and their application to inhaled particle deposition. *Bull. Math. Biol.* 42, 461–480. [https://doi.org/10.1016/S0092-8240\(80\)80060-7](https://doi.org/10.1016/S0092-8240(80)80060-7).
- Zhang, Y., Chia, T.L., Finlay, W.H., 2006. Experimental measurement and numerical study of particle deposition in highly idealized mouth-throat models. *Aerosol Sci. Tech.* 40, 361–372. <https://doi.org/10.1080/02786820600615055>.
- Zhao, Z., Xu, S., Wood, B.J., Tse, Z.T.H., 2018. 3D printing endobronchial models for surgical training and simulation. *J. Imaging* 4, 135. <https://www.mdpi.com/2313-433X/4/11/135>.